

Thermodynamic properties of excess-oxygen-doped $\text{La}_2\text{CuO}_{4.11}$ near a simultaneous transition to superconductivity and long-range magnetic order

G. A. Jorge,^{1,2,*} M. Jaime,¹ L. Civale,³ C. D. Batista,⁴ B. L. Zink,⁵ F. Hellman,⁵ B. Khaykovich,⁶ M. A. Kastner,⁶ Y. S. Lee,⁶ and R. J. Birgeneau⁷

¹National High Magnetic Field Laboratory, Los Alamos National Laboratory, Los Alamos, New Mexico 87545, USA

²Departamento de Física, Universidad de Buenos Aires, Pabellón 1 Ciudad Universitaria (1428), Buenos Aires, Argentina

³Superconductivity Technology Center, Los Alamos National Laboratory, Los Alamos, New Mexico 87545, USA

⁴Center for Non-Linear Studies, Los Alamos National Laboratory, Los Alamos, New Mexico 87545, USA

⁵Department of Physics, University of California, San Diego, La Jolla, California 92093, USA

⁶Department of Physics and Center for Material Science and Engineering, Massachusetts Institute of Technology, Cambridge, Massachusetts 02139, USA

⁷Department of Physics, University of Toronto, Toronto, Ontario, Canada M5S 1A7

(Received 29 August 2003; revised manuscript received 1 December 2003; published 28 May 2004)

We have measured the specific heat and magnetization versus temperature in a single crystal sample of superconducting $\text{La}_2\text{CuO}_{4.11}$ and in a sample of the same material after removing the excess oxygen, in magnetic fields up to 15 T. Using the deoxygenated sample to subtract the phonon contribution, we find a broad peak in the specific heat, centered at 50 K. This excess specific heat is attributed to fluctuations of the Cu spins possibly enhanced by an interplay with the charge degrees of freedom, and appears to be independent of magnetic field, up to 15 T. Near the superconducting transition $T_c(H=0)=43$ K, we find a sharp feature that is strongly suppressed when the magnetic field is applied parallel to the crystallographic c axis. A model for three-dimensional vortex fluctuations is used to scale magnetization measured at several magnetic fields. When the magnetic field is applied perpendicular to the c axis, the only observed effect is a slight shift in the superconducting transition temperature.

DOI: 10.1103/PhysRevB.69.174506

PACS number(s): 74.72.Dn, 74.40.+k, 75.30.Fv, 75.10.Jm

I. INTRODUCTION

The high-temperature cuprate superconductors are created by doping of Mott insulating materials, such as La_2CuO_4 , which show quasi-two-dimensional (2D) spin- $\frac{1}{2}$ antiferromagnetic (AFM) order. Neutron scattering experiments on La_2CuO_4 have shown instantaneous spin correlations in the copper-oxygen planes that persist to very high temperature because of the very strong in-plane exchange constant J .¹ Although the 3D AFM order, resulting from weak interplane coupling, is destroyed by doping of La_2CuO_4 , the in-plane dynamic correlations survive throughout the underdoped and superconducting portion of the phase diagram. Therefore, the interplay between the spin degrees of freedom and superconductivity is an important part of the current research on high- T_c superconductors.

Particularly interesting is the coexistence of static incommensurate spin density wave (SDW) order with superconductivity in several cuprates (for recent reviews, see Refs. 2, 3). Static SDW's were observed first in $\text{La}_{2-x-y}\text{Nd}_y\text{Sr}_x\text{CuO}_4$ (Ref. 4) and later in $\text{La}_{2-x}\text{Sr}_x\text{CuO}_4$, for x near $\frac{1}{8}$,⁵ and $\text{La}_2\text{CuO}_{4+y}$.⁶ Oxygen-doped $\text{La}_2\text{CuO}_{4+y}$ is most interesting in this respect not only because it has the highest $T_c=43$ K of entire doped La_2CuO_4 family of superconductors, but also because the transition to the superconductivity and the in-plane static long-range magnetic order coincide. According to neutron scattering and muon-spin rotation experiments, there is a well-defined phase transition to the magnetically ordered state at $T_m=T_c$.^{6,7} This magnetic order is two dimensional with the out-of-plane correlation

length of order 3 Cu-O planes. Above T_m , in the paramagnetic phase, there is evidence for long-coherence length and low-energy spin fluctuations.⁶ By applying a magnetic field, which suppresses the superconducting order parameter, the magnetic order parameter grows.⁸⁻¹⁰ This indicates that there is a competition between the magnetic order and superconductivity, in spite of the close proximity of T_m and T_c .

To learn more about the superconductivity and magnetism, we have measured the specific heat, in fields up to 15 T, and the magnetization, in fields up to 7 T, for $\text{La}_2\text{CuO}_{4.11}$. We have removed the excess oxygen from a piece of a similar oxygen-doped single crystal and have used its specific heat to estimate the phonon contribution. Subtraction of the latter reveals a broad peak near 50 K in the specific heat, which is insensitive to magnetic field and which we associate with spin fluctuations, enhanced by the involvement of charge degrees of freedom. In addition, there is narrow peak near the superconducting transition. The height and width of the latter peak, as well as its suppression by the magnetic field, is consistent with results for a Sr-doped $\text{La}_{2-x}\text{Sr}_x\text{CuO}_{4+y}$ superconductor of similar hole density. Analysis of the magnetization indicates strong 3D vortex fluctuations when the field is applied parallel to the c axis of the sample.

In the next section we discuss the experimental techniques (Sec. II A) and the sample preparation and characterization (Sec. II B). In Sec. III we present the results for specific heat (Sec. III A) and magnetization (Sec. III B) measurements. In Sec. IV we discuss the implication of our results, and a summary is presented in Sec. V.

II. EXPERIMENTAL DETAILS

A. Measurement techniques

The specific heat measurements were made with a thin silicon nitride (SiN) membrane microcalorimeter in fields applied parallel and perpendicular to the c axis by means of a superconducting magnet up to 15 T. The SiN membrane microcalorimeters consist in a silicon frame of $11 \times 11 \text{ mm}^2$ with a $5 \times 5 \text{ mm}^2$ SiN membrane, $1 \mu\text{m}$ thick. On the front side of the membrane there are a platinum resistor that works as a heater, and three different thermometers (one platinum resistor for high temperatures and two NbSi composite resistors for low temperatures).¹¹ On the back side of the membrane, a gold conduction layer is deposited in order to thermalize the thermometers and heater, and the sample is attached on it with a thermally conductive compound. These microcalorimeters have very low heat capacity addenda, allowing measurements of small samples (in the submilligram range), thin films¹¹ or small changes in specific heat of bulk samples when a small addenda is needed. Recent measurements¹² have proved that in these devices neither the membrane thermoconductance nor the addenda change significantly with fields up to 8 T, whereas our measurements show no change up to 15 T. The film thermometers on the membrane were calibrated in temperature and magnetic field against a factory-calibrated Cernox thermometer. The method used to measure specific heat is the thermal relaxation time technique.¹³ Magnetization measurements were performed in a commercial 7 T quantum design SQUID magnetometer, using a scan length of 4 cm (longitudinal magnetization), with fields applied parallel and perpendicular to the c axis.

B. Sample preparation and characterization

Single crystals of La_2CuO_4 have been grown by the traveling solvent floating zone technique and subsequently oxidized in an electrochemical cell, as described previously.⁶ Thermogravimetric analysis gives an oxygen excess of 0.11.^{6,9} We study a 3.06 mg piece of a single crystal of $\text{La}_2\text{CuO}_{4.11}$ of dimensions $0.6 \times 0.6 \times 1.4 \text{ mm}^3$, where the c axis is along the longer dimension. This is a small piece of the sample used in previous neutron scattering experiments.^{6,9}

The structure of La_2CuO_4 is shown in inset (a) of Fig. 1. The spin- $\frac{1}{2}$ Cu^{2+} ions order antiferromagnetically within the CuO_2 planes in the undoped material (as shown in the diagram). The c axis is perpendicular to the Cu-O planes. In oxygen-doped $\text{La}_2\text{CuO}_{4+y}$, the excess oxygen is intercalated between the Cu-O planes and forms a sine-density wave, which is periodic along the c axis. This behavior is called *staging*.¹⁴ Stage n corresponds to a period of n Cu-O layers. The sample studied here is predominantly in the stage-4 phase, which has its superconducting transition at $T_c = 43 \text{ K}$. The onset of static long-range magnetic order coincides with the onset of superconductivity.^{6,9} Note that $T_c = 43 \text{ K}$ is higher than that of optimally doped $\text{La}_{2-x}\text{Sr}_x\text{CuO}_4$, which is possibly due to the absence of quenched disorder from a random distribution of Sr^{2+} dop-

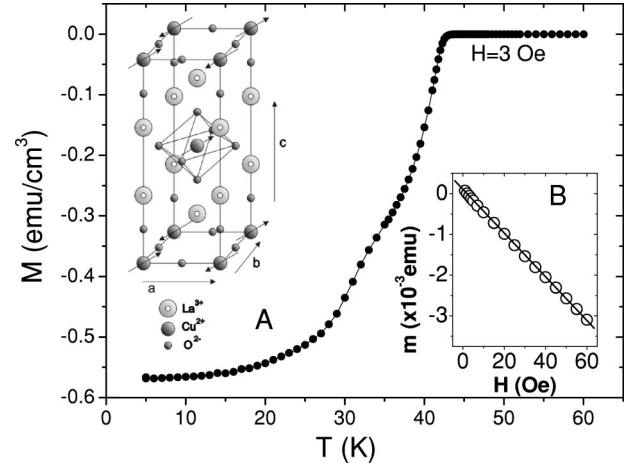


FIG. 1. Magnetization vs temperature at an applied field of 3 Oe. The onset of diamagnetic signal is at 43 K. The structure in the curve at lower temperatures probably indicates the presence of stage-6 phase. (a) Schematic structure of La_2CuO_4 , showing the spins of the copper ions. (b) Magnetic moment vs magnetic field at low fields (for $T = 5 \text{ K}$); the line is the result of a linear fit of the data. Both magnetization measurements were done after zero-field cooling.

ants. Previous neutron scattering experiments show no gap in the spin excitations in this sample.⁶

Our sample shows the onset of a diamagnetic signal at 43 K when measuring magnetization at an applied magnetic field of 3 Oe (see the main panel of Fig. 1). The structure observed in the magnetization at around 32 K almost certainly comes from inclusions of the stage-6 phase (less than 10% of the total volume) with $T_c = 32 \text{ K}$.

We have estimated the superconducting volume at 5 K from the slope of the magnetic moment vs field at low fields [inset (b) of Fig. 1], corrected by a demagnetization factor of $1/3$ for a sphere. The calculated volume is 0.45 mm^3 , close to the sample volume of 0.43 mm^3 , deduced from the sample mass. Although the superconducting volume calculated in this way can be affected by shielding effects, the height of the anomaly in the specific heat at the transition (see Sec. III A) indicates that in our sample the superconductivity is a bulk phenomenon and develops in the entire sample.

To create the deoxygenated sample we place another 0.5 mg piece of an oxygen-doped crystal in an Ar flow at 500°C for 2 h. This procedure eliminates the excess oxygen and results in undoped La_2CuO_4 material. We have used this sample to subtract the phonon background from the specific heat measurements, as discussed below. We note that the specific heat of the two samples agree very well at low temperatures without any adjustment.

III. RESULTS

A. Specific heat experiments

Figure 2(a) shows the specific heat data for the $\text{La}_2\text{CuO}_{4.11}$ single crystal as well as for the deoxygenated crystal of La_2CuO_4 , in zero field. The arrow indicates the

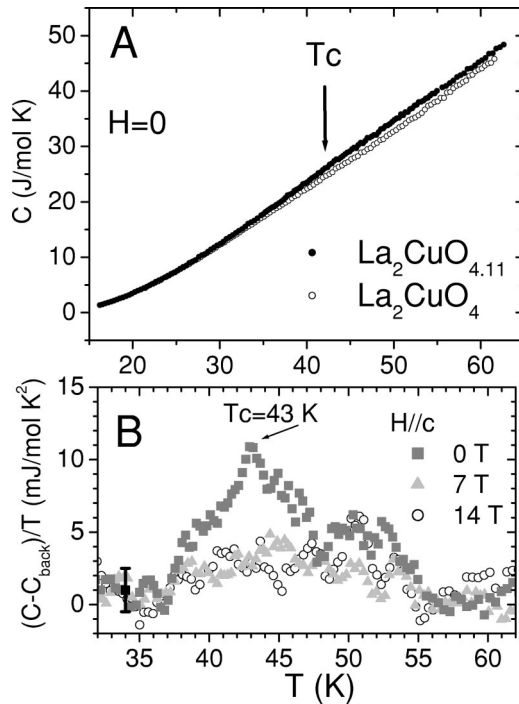


FIG. 2. (a) Specific heat vs Temperature at zero field for superconducting $\text{La}_2\text{CuO}_{4.11}$ and insulating La_2CuO_4 (their corresponding molar masses were used to calculate the specific heat per mole). The arrow indicates the position of the SC transition in the first curve. (b) Specific heat divided by T above the background at fields of 0, 7, and 14 T applied parallel to the c axis. The same background, linear in T , is subtracted from all three curves. The error bar shows the typical scattering of points ± 2 mJ/mol K^2 .

anomaly at the superconducting transition for the former. In order to clarify the contribution from superconductivity, we have subtracted a background (C_{back}) linear in T between 30 and 60 K from the original specific heat data. The measurements have been made at fields of 0, 7, and 14 T applied parallel to the c axis, and in Fig. 2(b) we plot the quantity $(C - C_{\text{back}})/T$ as a function of temperature. This is the method used previously to elucidate the specific heat anomaly at the transition.¹⁵⁻¹⁷ The peak at 43 K at zero field, with full width at half height of 5 K, corresponds to the onset of superconductivity. The height of the peak is 10 mJ/mole K^2 , which is only 2% of the total specific heat at 43 K. This peak height is consistent with other measurements of the specific heat in $\text{La}_2\text{CuO}_{4.093}$ (Ref. 17) and in $\text{La}_{1.85}\text{Sr}_{0.15}\text{CuO}_4$.^{16,18} When the field is applied parallel to the c axis of the sample, the anomaly is suppressed, as demonstrated by the curves for 7 and 14 T. At these fields, the peak has broadened and there is no clear sign of an anomaly over the entire temperature range measured.

In Fig. 3 we show the specific heat data in fields applied perpendicular to the c axis (in plane). We subtract, as before, a background linear in temperature between 30 and 60 K and divide by T . The curves are displaced for clarity. In this case the peak is present in all fields up to 15 T, with no change in height and a small shift towards lower temperatures with increasing fields (marked with a dashed line on the plot). The rate of change is 0.13 K/T.

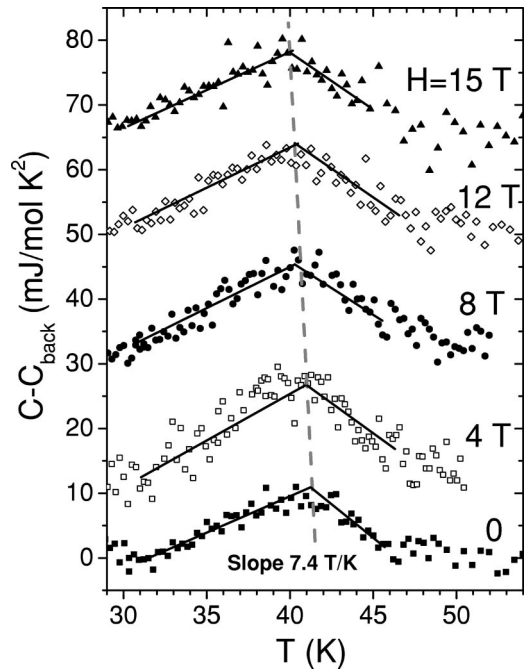


FIG. 3. Same as Fig. 2(b), with fields up to 15 T applied in plane. The curves are displaced for clarity, and straight lines are added as guides to the eye. The dashed line shows the shift of the SC transition with field.

Although the origin of the sharp peak at zero field in Fig. 2(b) and in fields applied perpendicular to the c axis in Fig. 3 is clearly identified with the superconducting transition, there is an extra contribution to the specific heat in the superconducting compound, evident from Fig. 2(a). The curve for the oxygenated sample departs from the deoxygenated one above 30 K. Subtracting the specific heat for the deoxygenated crystal, we obtain a plot of the excess of specific heat, shown in Fig. 4. The curves at the two fields match each other, except for the superconducting peak in the zero-field

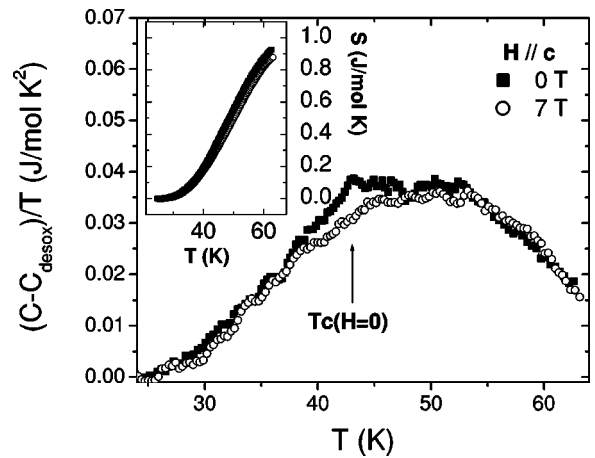


FIG. 4. Specific heat for $\text{La}_2\text{CuO}_{4.11}$ with that of the deoxygenated sample subtracted, for zero field and for a 7 T field applied parallel to the c axis. The superconducting transition is indicated with an arrow. The inset shows the entropy associated with the excess specific heat.

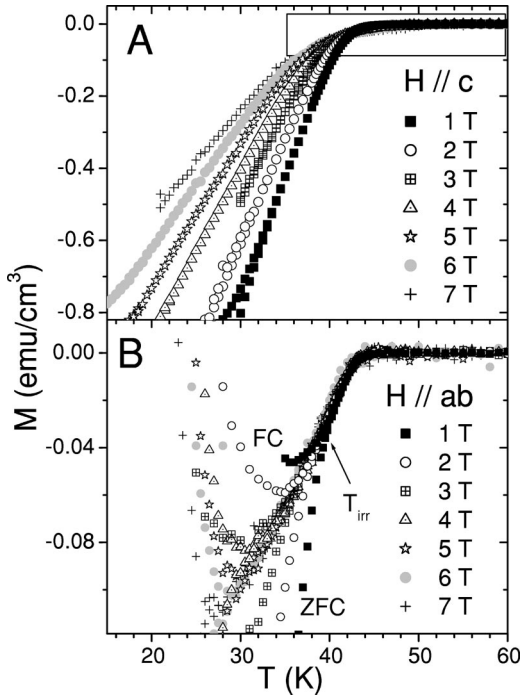


FIG. 5. Magnetization versus temperature curves for H parallel (a) and perpendicular (b) to the c axis. FC indicates curves taken while field cooling and ZFC curves taken while zero-field cooling. T_{irr} is the irreversibility temperature (shown for $H=1$ T). The rectangle is expanded in Fig. 6.

curve (indicated with an arrow). The inset of Fig. 4 shows the entropy associated with the excess specific heat obtained by numerical integration. The entropy at 65 K is 0.93 J/mol K, roughly 20% of the entropy expected for one spin- $\frac{1}{2}$ per Cu ion [$R \ln(2S+1)=5.76$ J/mol K].

B. Magnetization experiments

Magnetization measurements have been performed on the same single crystal used in the heat capacity studies for both orientations of the magnetic field. Figure 5 shows the data in fields applied parallel [panel (a)] and perpendicular [panel (b)] to the c axis. In the latter orientation, irreversible behavior is observed, and the zero field cooled (ZFC, lower curve) and field cooled (FC, upper curve) magnetization curves merge at the irreversibility temperature T_{irr} , shown on the figure for $H=1$ T. In the reversible region of the magnetization, curves at different fields are indistinguishable within the scatter of the points. This behavior is consistent with the specific heat results, which show only a slight displacement of the superconducting transition temperature with field.

For the field applied parallel to the c axis, panel (a) of Fig. 5 shows the reversible region of the magnetization up to 7 T. Note that the scale of the magnetization axis is 10 times than that in panel (b). We have expanded the region marked with a rectangle in Fig. 6. A clear crossing point is observed in curves up to 5 T (curves at 6 and 7 T are not plotted here). The characteristic temperature ($T^*=42.5$ K) and magnetization ($M^*=-0.023$ emu/cm 3) of this crossing point are

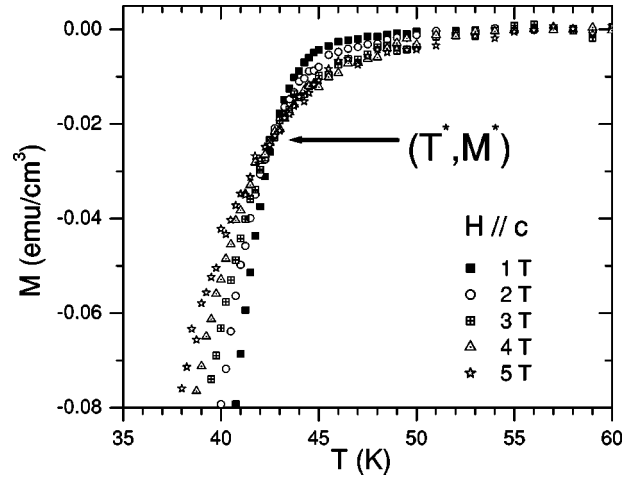


FIG. 6. Expansion of the rectangular region indicated in Fig. 5 ($H \parallel c$). The crossing point of these curves is a distinctive feature of vortex fluctuations. The characteristic temperature (T^*) and magnetization (M^*) are indicated.

marked on the graph. The crossing point in the magnetization vs temperature curves is a distinctive feature of vortex fluctuations.^{19–27}

IV. DISCUSSION

A. 2D spin fluctuations

We first discuss the specific heat results. One of the features in the specific heat of our superconducting sample $\text{La}_2\text{CuO}_{4.11}$ is the absence of a clear magnetic contribution at the simultaneous ordering temperature of 42–43 K. Indeed, we identified a small anomaly due to the superconducting transition. However, we did not observe any anomaly associated with the simultaneous onset of the static incommensurate magnetic order neither in the absence nor in the presence of the applied field of up to 15 T. This could be due to one of the following reasons: (a) the entropy recovered at the magnetic ordering temperature is quite small, as in the parent compound,²⁸ (b) the entropy is significant but distributed over a broad temperature range. Therefore, we measured a deoxygenated (insulating) sample of La_2CuO_4 to obtain the phonon contribution to the specific heat.

The insulating sample has two contributions to the specific heat at the low temperatures studied, one from the phonons and one from magnons. The magnon contribution (C_m) for undoped La_2CuO_4 was estimated from linear spin-wave theory for a 2D square lattice antiferromagnet to be²⁸

$$C_m = 2.385 \text{ J/mol K} \left(\frac{k_B}{J} \right)^2 T^2, \quad (1)$$

where k_B is the Boltzmann constant. Taking $J/k_B=1567$ K, Eq. (1) yields $C_m=1.8$ mJ/mol K at 40 K, a value that is four orders of magnitude less than the phonon contribution at that temperature (20 J/mol K), and well below the experimental resolution. We therefore can use the specific heat of

the deoxygenated sample as a background of phononic origin, leading to the plot of excess specific heat due to the doping shown in Fig. 4.

Doping La_2CuO_4 with oxygen leads to three effects which might contribute to the excess specific heat: (i) changes in the vibrational spectrum caused by excess oxygen, (ii) free carrier excitations, and (iii) changes in the spectrum of magnetic excitations. The staging of the interstitial oxygen is accompanied by a periodic reversal in the direction of the tilt of the CuO_6 octahedra along the c axis. This will likely cause a small change in the phonon spectrum. Changes in the phonon contribution of similar magnitude, but opposite sign, have been reported for $\text{YBa}_2\text{Cu}_3\text{O}_{6+x}$.²⁹ However, a direct comparison between these two systems is difficult because excess oxygen atoms occupy different sites in their crystal lattices: interstitials in $\text{La}_2\text{CuO}_{4+y}$ and chain sites in $\text{YBa}_2\text{Cu}_3\text{O}_{6+x}$. The broad peak is reminiscent of the Schottky anomaly for a system with a finite number of excited states, such as a spin- $\frac{1}{2}$ moment in a magnetic field. From the temperature of the peak we infer that, were such two-level systems responsible for the excess specific heat, the energy splitting of the two levels would be ~ 7 meV. We cannot exclude the possibility that the interstitial oxygens have a two-level systems associated with it, however, we think it is more likely that the excess specific heat is associated with a disordered component of the spin system, as discussed below.

The contribution to the specific heat from the free carriers must be small. Indeed, above T_c we use the BCS estimate $\gamma = \Delta C / 1.43 T_c \approx 6$ mJ/mol K^2 , far less than that observed.³⁰ In addition, free carriers are not expected to give a peak in the specific heat.

We suggest, instead, that the excess specific heat shown in Fig. 5 comes from a change in the spectrum of spin excitations resulting from the doping. The contribution of the spins to the specific heat in the 2D $S = \frac{1}{2}$ square lattice Heisenberg AFM [quantum Heisenberg antiferromagnet (QHA)] become important at temperatures of order the in-plane exchange constant J . Monte Carlo simulations of this model show that the heat capacity exhibits a broad peak at $k_B T \approx 0.6J$.^{27,31,32} Since the excess specific heat reported here is observed at 50 K, ascribing the excess specific heat to that of a QHA would imply that J is suppressed from ~ 135 to ~ 7 meV by doping. However, this conclusion contradicts results from neutron scattering. The instantaneous magnetic correlation length, measured by integrating over all the energies up to ~ 100 meV is almost constant as a function of temperature in the optimally doped or slightly underdoped $\text{La}_{2-x}\text{Sr}_x\text{CuO}_4$.¹ If J were in fact reduced by doping to 7 meV, then the correlation length would rise dramatically at low temperatures. Although the instantaneous correlation length has not been measured in oxygen-doped $\text{La}_2\text{CuO}_{4+y}$, its magnetic dynamics is very similar to slightly underdoped LSCO.⁶ Furthermore, we have measured the widths in q space of the magnetic fluctuation peaks associated with the SDW order and find no increase in their width up to ~ 9 meV. This allows us to place a lower bound on J in the superconductor of 60 meV.³³ We conclude that the excess specific heat is not described by the QHA with reduced J .

Neutron scattering results show that the ordered moment below the SDW transition increases dramatically with the application of a magnetic field.⁹ However, the excess specific heat, aside from the small component resulting from superconductivity, does not depend on the applied field. This and the absence of any critical behavior convince us that the observed anomaly cannot be attributed *only* to the fluctuations of the ordered magnetic moment near the SDW phase transition. We would not expect such a contribution since the nearest-neighbor spin correlations are already established at much higher temperatures, and hence there would not be enough excess entropy at 50 K to observe experimentally.

There is a connection between the excess specific heat and the frequency-dependent magnetic susceptibility $\chi''(\omega)$ measured with neutron scattering around the (π, π) point for slightly underdoped $\text{La}_{2-x}\text{Sr}_x\text{CuO}_4$. The latter shows a maximum as the energy transfer is lowered, at around 7 meV, before going to zero at lower energy. This maximum is most pronounced near the superconducting transition temperature.³⁴ This behavior shows that there is an enhancement of the (π, π) spin fluctuations at ~ 7 meV in $\text{La}_{2-x}\text{Sr}_x\text{CuO}_4$ of similar hole density to the $\text{La}_2\text{CuO}_{4.11}$ sample studied here. The susceptibility around (π, π) of $\text{La}_2\text{CuO}_{4.11}$ does not show such a maximum, but rather is approximately constant at low energies. For the latter material $\chi''(\omega)$ is enhanced at low energies relative to that in $\text{La}_{2-x}\text{Sr}_x\text{CuO}_4$ because of the magnons associated with the static long-range-ordered incommensurate SDW. However, muon measurements indicate that the local magnetic order is fully developed microscopically at only about 40% of the muon sites.^{7,9} The remaining 60% of the sample, which has a very small ordered moment, is likely to have spin excitations closely similar to those in $\text{La}_{2-x}\text{Sr}_x\text{CuO}_4$ ($x=0.14$) and should exhibit the enhanced spin fluctuations at around 7 meV. We speculate, therefore, that the broad anomaly in the specific heat reflects the enhanced magnetic fluctuations coming from the disordered 2D spin- $\frac{1}{2}$ system.

Naively, one expects the entropy associated with these fluctuations to be even smaller than the contribution from the moments that order below 42 K. Consequently, the large enhancement of spin fluctuations observed in the experiments must be the result of an interplay between charge and spin degrees of freedom. The relevant energy scale for the charge degrees of freedom is given by the superconducting transition temperature $T_c = 43$ K, close to the temperature at which the excess specific heat is observed.

B. Superconducting transition

We next discuss the behavior of the magnetization and specific heat near the superconducting transition. Vortex fluctuations (fluctuations in the position of vortex lines) in high temperature superconductors have been observed in $\text{Bi}_2\text{Sr}_2\text{CaCu}_2\text{O}_8$,^{19,20} $\text{YBa}_2\text{Cu}_3\text{O}_{7-\delta}$,^{21,24} and $\text{La}_{2-x}\text{Sr}_x\text{CuO}_4$ (Refs. 25,26) among others. Several theoretical studies, based on the Ginzburg-Landau (GL) free energy, explain the appearance of the crossing point T^* where the magnetization M^* is independent of the field.^{22,23} From the

values of T^* and M^* we estimate the correlation length along the c axis for the vortex fluctuations, using the expression in Refs. 22 and 23

$$-M^* = -M(T^*) = \frac{k_B T^*}{\Phi_0 l_c} A, \quad (2)$$

where k_B is the Boltzmann constant, Φ_0 is the flux quantum, l_c the correlation length for the fluctuations, and the constant A is set to 1. In our case, the correlation length we find, $l_c \approx 125 \text{ \AA}$, is almost 20 times the distance between planes ($\sim 7 \text{ \AA}$), which suggests that the fluctuations in our system have 3D character. For comparison, the correlation length for $\text{La}_{2-x}\text{Sr}_x\text{CuO}_4$ with a Sr content $x=0.14$ is $l_c \approx 60 \text{ \AA}$, deducted from the data in Ref. 26. This value is half the correlation length in our sample. Also we found that the penetration depth $\lambda_0 = \lambda_{ab}(T=0)$ is larger for our material than for the compound doped with Sr. We estimate the penetration depth for our sample from magnetization vs magnetic field curves²² (that we measured separately but do not include in this paper) to be $\lambda_0 \approx 3800\text{--}4000 \text{ \AA}$. This value is in agreement with a previous estimation on powdered $\text{La}_2\text{CuO}_{4+y}$ ($y \leq 0.13$), which gives $\lambda_0 \approx 4200 \text{ \AA}$.³⁵ For the compound doped with Sr ($x=0.15$), $\lambda_0 \approx 2000\text{--}2500 \text{ \AA}$.^{36,37}

Several physical properties show scaling behavior when critical fluctuations dominate.³⁸ In particular, magnetization vs temperature curves taken at different fields are expected to collapse to a single function when the variables

$$\frac{M}{(TH)^s} \text{ vs } \frac{[T-T_c(H)]}{(TH)^s} \quad (3)$$

are plotted.^{21,24,26} Here the exponent s is $\frac{1}{2}$ for 2D fluctuations and $\frac{2}{3}$ for 3D behavior. The function $T_c(H)$, the transition temperature as a function of field, is chosen in order to optimize the scaling.

Figure 7 shows the scaling of the variables in Eq. (3) for 3D [panel (a)] and 2D [panel (b)] vortex fluctuations, in fields up to 5 T. The differences between the curves for the 2D case are appreciable, and we are not able to find a $T_c(H)$ function that makes the different curves collapse. In contrast, panel A shows 3D scaling, for which all the curves up to 5 T scale within experimental error. The inset in Fig. 7 shows the function $T_c(H)$ used in the scaling. Curves at 6 and 7 T were not included in Fig. 7A because they start deviating from the other curves, presumably due to a departure from the scaling behavior.

Figure 7 indicates that our system shows 3D vortex fluctuations in fields applied parallel to the c axis up to 5 T. The fundamental parameter governing the strength of the thermal fluctuations is the Ginzburg number $G_i = [T_c/H_c^2(0)\varepsilon\xi^3(0)]^2/2$, where H_c is the thermodynamic critical field, ε the anisotropy parameter, and ξ the GL coherence length.³⁹ Based on the superconducting parameters found for our sample we can estimate a Ginzburg number $G_i \approx 0.07$, which, together with the transition temperature $T_c = 42 \text{ K}$, yields a critical region $\Delta T = G_i T_c \approx 3 \text{ K}$ wide. This fact is reflected in the plots of Fig. 7, where a region of roughly the size of the fluctuations range is shown. In higher

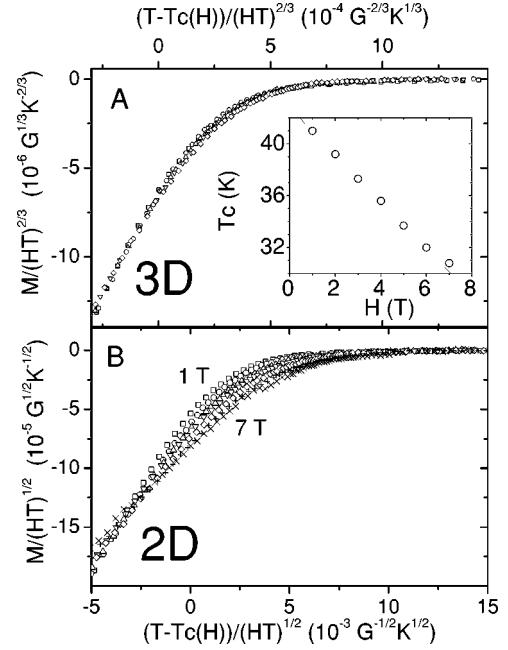


FIG. 7. Scaling of the magnetization data in the variables (3), for 3D (a) and 2D (b) vortex fluctuations. The scaling works for presumed 3D fluctuations up to 5 T. Inset: Function $T_c(H)$ used in the 3D scaling. All the curves are ZFC.

fields the fluctuations are still present but their dimensionality becomes obscure, possibly related to a 3D to 2D crossover at high fields,^{25,39} although this point requires more investigation.

As we mentioned earlier, such scaling of magnetization is very common to different high- T_c cuprates, including $\text{Bi}_2\text{Sr}_2\text{CaCu}_2\text{O}_8$, $\text{YBa}_2\text{Cu}_3\text{O}_{7-\delta}$, and $\text{La}_{2-x}\text{Sr}_x\text{CuO}_4$. We also point out that the 3D nature of the flux lines serves as another confirmation of the doping homogeneity of our material. Despite the oxygen-density modulation associated with staging, based on the results of neutron and NMR measurements we know that the degree of doping in the Cu-O layers is as homogeneous as in the best samples of $\text{La}_{2-x}\text{Sr}_x\text{CuO}_4$.^{6,9} The existence of 3D flux lines with correlation length of 20 Cu-O layers serves as an additional confirmation of this conclusion.

The disappearance of the specific heat peak at the superconducting transition with a magnetic field parallel to the c axis has been universally observed in cuprate superconductors.^{18,40–43} Several mechanisms have been proposed to account for this effect, such as the possible two-dimensional nature of the superconducting phase transition in layered cuprates, effective one-dimensional character of the transition in the presence of the field because the quasiparticles are bound to the lowest Landau level in the field, or finite size effects (see, for example, Ref. 21, and references therein). All these effects are anisotropic and result in suppression of the transition by the field parallel to the c axis.

For completeness, in Fig. 8 we present the phase diagram constructed from magnetization data. The irreversibility line is taken from the merging of the ZFC and FC data, the H_{c2} line for $H\parallel c$ is taken from the scaling (inset of Fig. 7), and

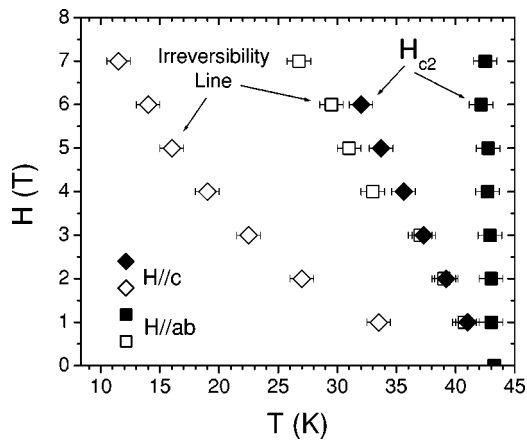


FIG. 8. Phase diagram from the magnetization experiment. Open symbols represent irreversibility line, and solid symbols H_{c2} . Squares are for $H_{\perp c}$ and diamonds for $H_{\parallel c}$.

the H_{c2} line for $H_{\perp c}$ from the extrapolation of the reversible magnetization to zero. Note that we have found very similar values of $H_{c2}(T)$ ($H_{\parallel c}$) from the transport measurements on the same sample.⁹

V. SUMMARY

We have presented specific heat and magnetization measurements on a single crystal of $\text{La}_2\text{CuO}_{4.11}$, in magnetic fields up to 15 T. A broad peak centered at 50 K is observed in the specific heat measurements when the specific heat of a

deoxygenated sample is subtracted. We attribute this peak to fluctuations in the disordered spin system associated with the optimally doped and underdoped superconductors. The effect of these fluctuations is possibly enhanced by an interplay between the charge and spin degrees of freedom. At the superconducting transition, we find that a sharp specific heat peak associated with the onset of the superconducting state is dramatically broadened, when the field was parallel to the c axis. Our magnetization measurements show evidence of strong vortex fluctuations with a correlation length of 20 Cu-O planes. 3D scaling fits the data well with a linear H_{c2} curve up to 5 T.

Note added in proof. In a recent work by Lee *et al.*,⁴⁴ the authors report the effect of disorder caused by excess oxygen. They find that the quenched disorder enhances the spin-density wave order in a manner analogous to the effects of an applied magnetic field.

ACKNOWLEDGMENTS

We thank V. Bekeris for a critical reading of the manuscript. Work at the NHMFL was performed under the auspices of the National Science Foundation (Grant No. DMR90-16241), The State of Florida, and the U.S. Department of Energy. Work at MIT was supported primarily by the MRSEC Program of the National Science Foundation under Grant No. DMR 02-13282. Research at the University of Toronto was supported by the Natural Science and Engineering Research Council of Canada.

*Email address: gjorge@df.uba.ar

¹M.A. Kastner, R.J. Birgeneau, G. Shirane, and Y. Endoh, *Rev. Mod. Phys.* **70**, 897 (1998).

²S.A. Kivelson, E. Fradkin, V. Oganesyan, I.P. Bindloss, J.M. Tranquada, A. Kapitulnik, and C. Howald, *cond-mat/0210683*.

³S. Sachdev, *Rev. Mod. Phys.* **75**, 913 (2003).

⁴J.M. Tranquada, B.J. Sternlieb, J.D. Axe, Y. Nakamura, and S. Uchida, *Nature (London)* **375**, 561 (1995).

⁵H. Kimura, K. Hirota, H. Matsushita, K. Yamada, Y. Endoh, S.-H. Lee, C.F. Majkrzak, R. Erwin, G. Shirane, M. Greven, Y.S. Lee, M.A. Kastner, and R.J. Birgeneau, *Phys. Rev. B* **59**, 6517 (1999).

⁶Y.S. Lee, R.J. Birgeneau, M.A. Kastner, Y. Endoh, S. Wakimoto, K. Yamada, R.W. Erwin, S.-H. Lee, and G. Shirane, *Phys. Rev. B* **60**, 3643 (1999).

⁷A.T. Savici, Y. Fudamoto, I.M. Gat, T. Ito, M.I. Larkin, Y.J. Uemura, G.M. Luke, K.M. Kojima, Y.S. Lee, M.A. Kastner, R.J. Birgeneau, and K. Yamada, *Phys. Rev. B* **66**, 014524 (2002).

⁸S. Katano, M. Sato, K. Yamada, T. Suzuki, and T. Fukase, *Phys. Rev. B* **62**, R14677 (2000).

⁹B. Khaykovich, Y.S. Lee, R.W. Erwin, S.H. Lee, S. Wakimoto, K.J. Thomas, M.A. Kastner, and R.J. Birgeneau, *Phys. Rev. B* **66**, 014528 (2002).

¹⁰B. Lake, H.M. Ronnow, N.B. Christensen, G. Aeppli, K. Lefmann, D.F. McMorrow, P. Vorderwisch, P. Smeibidl, N. Mangkorntong, T. Sasagawa, H. Takagi, and T.E. Mason, *Nature (London)* **415**, 299 (2002).

¹¹D.W. Denlinger, E.N. Abarra, K. Allen, P.W. Rooney, M.T. Messer, S.K. Watson, and F. Hellman, *Rev. Sci. Instrum.* **65**, 946 (1994).

¹²B.L. Zink, B. Revaz, R. Sappéy, and F. Hellman, *Rev. Sci. Instrum.* **73**, 1841 (2002).

¹³R. Bachmann, F.J. DiSalvo, T.H. Geballe, R.L. Greene, R.E. Howard, C.N. King, H.C. Kirsch, K.N. Lee, R.E. Schwall, H.-U. Thomas, and R.B. Zubeck, *Rev. Sci. Instrum.* **43**, 205 (1972).

¹⁴B.O. Wells, Y.S. Lee, M.A. Kastner, R.J. Christianson, R.J. Birgeneau, K. Yamada, Y. Endoh, and G. Shirane, *Science* **277**, 1067 (1997).

¹⁵A. Migliori, W. Visscher, S.E. Brown, Z. Fisk, S.W. Cheong, B. Alten, E.T. Ahrens, K.A. Kubat-Martin, J.D. Maynard, Y. Huang, D.R. Kirk, K.A. Gillis, H.K. Kim, and M.H.W. Chan, *Phys. Rev. B* **41**, 2098 (1990).

¹⁶A.M. Balbashev, D.A. Shulyatev, G.K. Panova, M.N. Khlopkin, N.A. Chernoplekov, A.A. Shikov, and A.V. Suetin, *Physica C* **256**, 371 (1996).

¹⁷T. Hirayama, M. Nakagawa, and Y. Oda, *Solid State Commun.* **113**, 121 (2000).

¹⁸R.A. Fisher, N.E. Phillips, A. Schilling, B. Buffeteau, R. Calemczuk, T.E. Hargreaves, C. Marcenat, K.W. Dennis, R.W. McCallum, and A.S. O'Connor, *Phys. Rev. B* **61**, 1473 (2000).

¹⁹K. Kadowaki, *Physica C* **185-189**, 2249 (1991).

²⁰P.H. Kes, C.J. van der Beek, M.P. Maley, M.E. McHenry, D.A. Huse, M.J.V. Menken, and A.A. Menovsky, *Phys. Rev. Lett.* **67**, 2383 (1991).

- ²¹U. Welp, S. Fleshler, W.K. Kwok, R.A. Klemm, V.M. Vinokur, J. Downey, B. Veal, and G.W. Crabtree, *Phys. Rev. Lett.* **67**, 3180 (1991).
- ²²L.N. Bulaevskii, M. Ledvij, and V.G. Kogan, *Phys. Rev. Lett.* **68**, 3773 (1992).
- ²³Z. Tesanovic, L. Xing, L. Bulaevskii, Q. Li, and M. Suenaga, *Phys. Rev. Lett.* **69**, 3563 (1992).
- ²⁴A. Wahl, V. Hardy, F. Warmont, A. Maignan, M.P. Delamare, and C. Simon, *Phys. Rev. B* **55**, 3929 (1997).
- ²⁵J. Mosqueira, J.A. Campá, A. Maignan, I. Rasines, A. Revcolevschi, C. Torrón, J.A. Veira, and F. Vidal, *Europhys. Lett.* **42**, 461 (1998).
- ²⁶Y.M. Huh and D.K. Finnemore, *Phys. Rev. B* **65**, 092506 (2002).
- ²⁷I.M. Sutjahja, A.A. Nugroho, M.O. Tjia, A.A. Menovsky, and J.J.M. Franse, *Phys. Rev. B* **65**, 214528 (2002).
- ²⁸K. Sun, J.H. Cho, F.C. Chou, W.C. Lee, L.L. Miller, D.C. Johnston, Y. Hidaka, and T. Murakami, *Phys. Rev. B* **43**, 239 (1991).
- ²⁹J.W. Loram, K.A. Mirza, J.R. Cooper, and W.Y. Liang, *Phys. Rev. Lett.* **71**, 1740 (1993).
- ³⁰M. Tinkham, *Introduction to Superconductivity* (McGraw-Hill, New York, 1996).
- ³¹G. Gomez-Santos, J.D. Joannopoulos, and J.W. Negele, *Phys. Rev. B* **39**, 4435 (1989).
- ³²P. Sengupta, A.W. Sandvik, and R.R.P. Singh, cond-mat/0306046 (unpublished).
- ³³Y. S. Lee, S. Wakimoto, and R. J. Birgeneau (unpublished).
- ³⁴G. Aeppli, T.E. Mason, S.M. Hayden, H.A. Mook, and J. Kulda, *Science* **278**, 1432 (1997).
- ³⁵E.J. Ansaldo, J.H. Brewer, T.M. Riseman, J.E. Schirber, E.L. Venturini, B. Morosin, D.S. Ginley, and B. Sternlieb, *Phys. Rev. B* **40**, 2555 (1989).
- ³⁶W.J. Kossler, J.R. Kempton, X.H. Yu, H.E. Schone, Y.J. Uemura, A.R. Moodenbaugh, M. Suenaga, and C.E. Stronach, *Phys. Rev. B* **35**, 7133 (1987).
- ³⁷G. Aeppli, R.J. Cava, E.J. Ansaldo, J.H. Brewer, S.R. Kreitzman, G.M. Luke, D.R. Noakes, and R.F. Kiefl, *Phys. Rev. B* **35**, 7129 (1987).
- ³⁸S. Ullah and A.T. Dorsey, *Phys. Rev. B* **44**, 262 (1991).
- ³⁹G. Blatter, M.V. Feigel'man, V.B. Geshkenbein, A.I. Larkin, and V.M. Vinokur, *Rev. Mod. Phys.* **66**, 1125 (1994).
- ⁴⁰S.E. Inderhees, M.B. Salamon, J.P. Rice, and D.M. Ginsberg, *Phys. Rev. Lett.* **66**, 232 (1991).
- ⁴¹O. Jeandupeux, A. Schilling, H.R. Ott, and A. van Otterlo, *Phys. Rev. B* **53**, 12 475 (1996).
- ⁴²A. Carrington, A.P. Mackenzie, and A. Tyler, *Phys. Rev. B* **54**, R3788 (1996).
- ⁴³A. Junod, A. Erb, and C. Renner, *Physica C* **317-318**, 333 (1999).
- ⁴⁴Y.S. Lee, F.C. Chou, A. Tewary, M.A. Kastner, S.H. Lee, and R.J. Birgeneau, *Phys. Rev. B* **69**, 020502(R) (2004).